Electronic properties, stability, and length scales of Cs_N clusters

1999 J. Phys.: Condens. Matter 11 1

(http://iopscience.iop.org/0953-8984/11/1/002)

J. Phys.: Condens. Matter **11** (1999) 1–18. Printed in the UK PII: S0953-8984(99)94590-3

Electronic properties, stability, and length scales of Cs_N clusters

Michael Springborg

Department of Chemistry, University of Konstanz, D-78457 Konstanz, Germany

Received 27 May 1998, in final form 2 September 1998

Abstract. Three basically different models of Cs_N clusters are studied, partly in order to explore the limitations of each model and partly in order to study general ground-state properties of the clusters. One model is based on the spherical-jellium model within the density-functional formalism, another is a semi-empirical tight-binding model obtained by parametrizing band structures for an infinite crystal, and the third model is a spherical-well model for non-interacting particles. Particularly stable clusters are found for systems with only completely filled electronic shells, although this result is somewhat obscured by surface effects for the tight-binding model. For the density of states as a function of N the tight-binding model is the one providing the most accurate information, especially for the features closest to the Fermi level. Only this model gives the proper description of those in the limit $N \rightarrow \infty$. Finally, we examine the electron density for different clusters and explore how Friedel oscillations occur. In particular the jellium model predicts very regular density oscillations, which can be ascribed to electron–electron interactions. We study both the pure clusters and ones with a void at the centre, where the latter represents a simple model for Cs-covered C_{60} molecules. The two systems show many similarities—in particular it is demonstrated that the stable clusters occur with the same spacing ΔR of the radius of the system. The cluster sizes range up to values of N of about 10 000 for the jellium and the tight-binding models and to over 30 000 for the spherical-well model. In total the study shows that although many properties are well described by all of the models, it is important to be aware of their limitations, and it would be desirable to incorporate more experimental information in order to be able to evaluate the quality of the different models. To this end the 'magic numbers' are less convenient.

1. Introduction

Clusters are intermediates between molecules and solids. Often they consist of only one type of atom and the number N of atoms lies typically in the range 10–10 000. Furthermore, they are often for N larger than some 10s close to spherically symmetric.

Their interesting properties originate partly from the fact that the number of atoms at the surface relative to N is large and partly from finite-size or quantum-confinement effects. Obviously, they have been the focus of several experimental and theoretical studies during the last roughly 15 years (see references [1, 2] for detailed reviews).

One of the central questions is how the properties depend on N. Theoretical studies suffer from the problem that the systems are large without being treatable as infinite and periodic. Simultaneously, they contain many inequivalent atoms. This makes *ab initio* methods prohibitively involved for N larger than $\sim$50. Therefore, current theoretical descriptions are based on several approximations. First, only the valence electrons are considered. Second, often the structure is taken as that of the crystalline material.

0953-8984/99/010001+18$19.50

When calculating the total energy $E_{\rm tot}$ as a function of N one may furthermore apply a tight-binding approximation for the electronic hopping integrals and subsequently approximate $E_{\rm tot}$ by the sum of the single-particle energies of the occupied orbitals. This amounts to assuming that electronic effects determine the properties of the clusters. Such approaches have been undertaken by Mansikka-aho *et al* [3, 4] and by Lindsay *et al* [5] for N up to about 1000. In the earlier papers [3, 5] the simplest Hückel model was applied, but more recently [4] a more accurate tight-binding model explicitly developed for Na clusters was employed. Here, we shall report results of such tight-binding studies for clusters with up to more than 10 000 atoms and we shall apply a tight-binding model that is explicitly developed for the element of interest to us, Cs.

Another often-applied approximation is the jellium approximation [6–18]. Thereby a true spherical symmetry can be obtained and the electronic properties can be calculated within the density-functional formalism of Hohenberg, Kohn, and Sham [19, 20]. As an improvement, Martins *et al* [7] and Lermé *et al* [21] included also the effects of the positions of the nuclei in an averaged way.

It turns out that the single-particle potential felt by the electrons has a simple and partly universal shape independent of the size of the system. Therefore, simple studies considering non-interacting particles moving in a given potential have been reported, too [21,23–27]. Since this potential is approximately a constant inside the cluster for larger systems, the simplest approximation amounts to assuming that the potential is constant inside the cluster and infinite outside.

The three approaches are based on different assumptions and it is far from clear that for a given material they will predict the same properties. Although this is a very important question when using any of the three models in analysing experimental results, it has not been addressed previously. It is the purpose of the present paper to present results of a such study. We shall here concentrate on ground-state properties, although the models are often used also in studying excitations. Furthermore, deviations from spherical symmetry may occur in real systems but here we shall only consider clusters that are close to spherically symmetric. Thereby the comparison between the three models is optimal.

We have used all three approaches for Cs clusters as a prototype. In section 2 we describe our theoretical methods, i.e., the density-functional jellium model, the tight-binding model, and the spherical-well model. In section 3 we present our results for pure Cs_N clusters. A more complicated system is treated in section 4. This system is essentially a spherical cluster with a void at the centre and represents the simplest approximation for Cs atoms deposited on a C_{60} molecule. Thus, the C_{60} molecule is responsible for the void. Finally, we conclude in section 5.

2. Theoretical models

2.1. The jellium model

Within the jellium model we apply the density-functional formalism of Hohenberg, Kohn, and Sham [19, 20]. Exchange and correlation effects are included via the local approximation of von Barth and Hedin [28]. Only one valence electron per atom is included and the jellium background density is assumed spherically symmetric and described by the electron-gas parameter $r_s = 5.62$ au, i.e., one particle per volume of $\frac{4\pi}{3}r_s^3$. This value of r_s corresponds to the density in crystalline Cs. The resulting one-dimensional single-particle equations are solved numerically, whereby both the orbitals, their single-particle energies, and the total energy are obtained.

2.2. The tight-binding model

For N not too small the clusters are close to spherically symmetric and can be considered fragments of the crystalline material. Cs crystallizes in the bcc structure with a lattice constant $a = 11.41$ au. Assuming that Cs has only one valence electron per atom we may describe its electronic properties through the (single-particle) model Hamiltonian

$$\hat{H}_{\mathrm{tb}} = \sum_{i,j} t_{ij} \hat{c}_i^{\dagger} \hat{c}_j \tag{1}$$

where $\hat{c}_i^{\dagger}$ ($\hat{c}_i$) creates (annihilates) an electron on site i. t_{ij} is the hopping integral that in the present case only depends on the distance between atoms i and j.

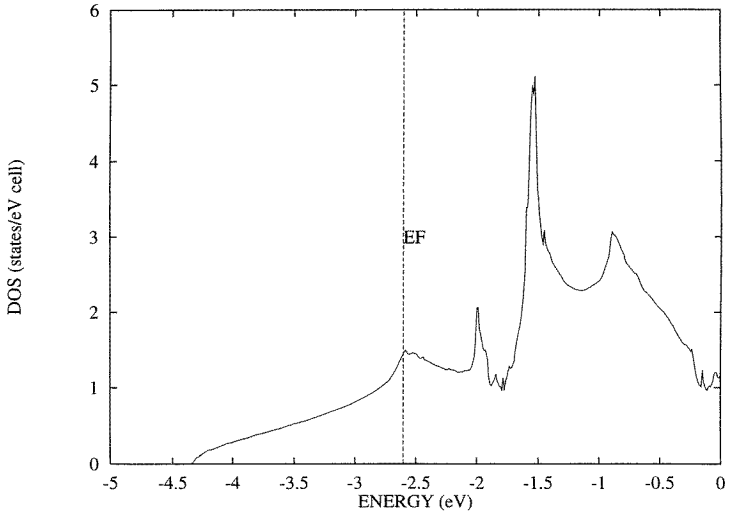

Figure 1. The density of states for crystalline Cs as calculated with the LMTO-ASA method. Only the 6s valence electrons were included in the calculation, whereas all other electrons were treated within a frozen-core approximation. The Fermi energy ϵ_F is marked by the vertical dashed line.

In order to determine t_{ij} we performed density-functional LMTO-ASA [29] calculations on crystalline Cs with the experimental lattice constant. The resulting density of states is shown in figure 1 and is seen to resemble that of a free-electron gas up to about 0.5 eV below the Fermi level ϵ_F, but with some deviations from the free-electron behaviour around ϵ_F.

The band energies of the occupied bands at a few high-symmetry points were subsequently fitted with those of the Hamiltonian of equation (1), which resulted in $t_{ij} = -0.146$ eV, -0.115 eV, and 0.022 eV for first-, second-, and third-nearest-neighbour interactions, respectively. For our purposes the on-site terms t_{ii} are uninteresting and therefore ignored (see, however, section 3.1). Further interactions were not included which is justified considering the smallness of the third-nearest-neighbour hopping integrals.

Also Mansikka-aho *et al* [4] applied a tight-binding model, but for Na clusters. They, however, assumed that the band structures of the infinite crystal are free-electron-like which may not be exactly the case.

For the clusters we use the Hamiltonian of equation (1) with the only difference being that i and j are allowed to run only over the sites within a pre-defined distance R from a given central atom. This corresponds to generating clusters of different sizes by subsequently adding

more and more 'atomic' shells. Here, we have considered clusters with up to 161 atomic shells, i.e. up to $N = 11\,017$.

From the Schrödinger single-particle equation

$$\hat{H}_{\mathrm{tb}}\psi_i = \epsilon_i \psi_i \tag{2}$$

we define the electronic energy

$$E_{\mathrm{tb}} = \sum_i n_i \epsilon_i \tag{3}$$

with n_i being the occupancies.

E_{tb} contains a term that is proportional to the size of the system as well as one that is proportional to the size of the surface. By studying the excess energy

$$E_{\mathrm{exc}} = E_{\mathrm{tb}} - aR^3 - bR^2 \tag{4}$$

we can therefore focus on those electronic effects that are beyond those of volume and surface effects. a and b in equation (4) are obtained through a least-squares fit of E_{tb} for a larger set of different values of R.

2.3. The spherical-well model

It is useful to consider also the simple model of non-interacting particles confined to the interior of a sphere of radius R. For this system the single-particle energies ϵ_{nl} are defined through

$$j_l\left(\sqrt{\frac{2m}{\hbar^2}\epsilon_{nl}}R\right) = 0 \tag{5}$$

with j_l being the lth spherical Bessel function of the first kind.

Also in this case we define a system of a certain size R containing N particles. Here,

$$N\frac{4\pi}{3}r_s^3 = \frac{4\pi}{3}R^3. \tag{6}$$

An electronic energy and an excess energy such as those defined in equations (3) and (4) will also be considered in this case.

This model is equivalent to the infinite-barrier model of Ekardt *et al* [22].

3. Results

3.1. Relative stability

The total energy per atom of the jellium calculations (figure 2(a)) for $1 \leqslant N \leqslant 310$ shows the well-known local minima (see, e.g., references [1, 2]) that can be ascribed to the filling of single or groups of energetically nearly degenerate electronic shells (cf. figure 3). In figure 3 we observe that the orbital energy as a function of N for a given orbital is not a monotonic function but shows some small discontinuities. These occur mainly at the positions where also the Fermi level makes a jump and indicate that all electrons feel the effects of completing the (n, l) shells. Moreover, for not too small N, the orbitals tend to group together with the result that the local minima in figure 2(a) occur not every time a single (n, l) shell is filled but rather when such a group is filled.

In figure 2(a) it is clear that the magic clusters appear at regular R-intervals, as has been observed by others (see, e.g., references [2,27]). For later purpose we show in table 1 the sizes of the magic clusters together with those (n, l) shells that are filled for a given size.

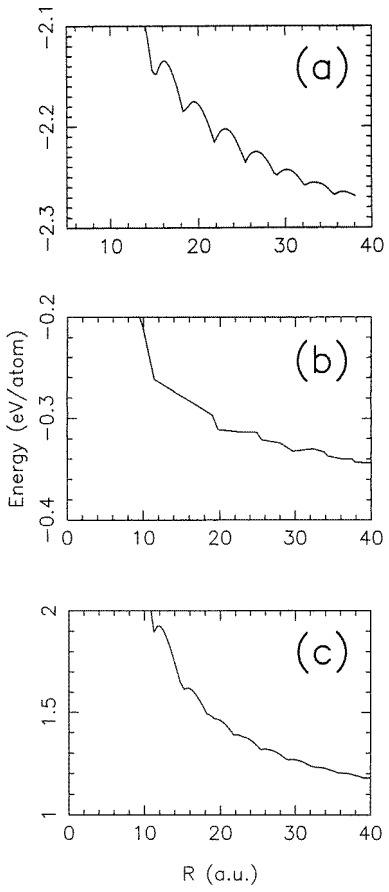

Figure 2. (*a*) The total energy per atom for the jellium model as a function of the radius R of the cluster. (*b*) As (*a*) but for the tight-binding model. (*c*) As (*a*) but for the spherical-well model.

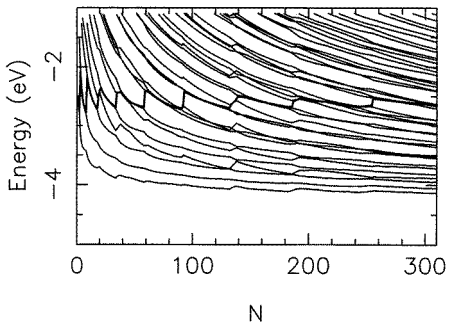

Figure 3. The single-particle eigenvalues for the jellium model as functions of N. The thicker line shows the energy of the highest occupied orbital.

For the spherical-well model one obtains the relative total energy shown in figure 2(*c*). Comparing with figure 2(*a*) we observe local energy minima for exactly the same cluster sizes. However, the local minima are more pronounced in the density-functional calculations than in the spherical-well model. Since the main difference of the two systems is the electron–electron interactions, we will ascribe the differences between figures 2(*a*) and 2(*c*) to those.

The spherical-well model has one important property. Independently of the size of the well (i.e., of R) the eigenvalues appear in the same order. For this model, the eigenvalues as functions of N are accordingly proportional to $N^{-2/3}$ (cf. equations (5) and (6)). This behaviour is recovered only approximately in figure 3, supporting the hypothesis that the irregularities in figure 3 are due to electron–electron interactions.

As is well known, the positions of the local minima in figure 2(*c*) can be explained with the help of the theory of Balian and Bloch [30] according to which (groups of) closed shells for a spherical system appear with regular intervals of

$$\Delta R = 0.603 r_s \tag{7}$$

Table 1. The values N for the clusters where the jellium calculations predict closed electronic shells and, equivalently, local minima in the total energy per atom. For a given N in the table all orbitals with the (n, l) up to and including the values listed are completely filled. In contrast to the case for atomic physics, $n - 1$ gives the number of radial nodes, and not the total number of nodes. In some cases more (n, l) shells are nearly degenerate and essentially filled simultaneously. Also given in the table are the radii of the closed-shell clusters.

N	(n, l)				R (au)
2	(1, 0)				7.08
8	(1, 1)				11.24
18	(1, 2)				14.73
20	(2, 0)				15.26
34	(1, 3)				18.21
58	(2, 1)	(1, 4)			21.75
92	(2, 2)	(1, 5)	(3, 0)		25.37
132	(2, 3)	(1, 6)			28.62
138	(3, 1)				29.04
186	(1, 7)	(2, 4)			32.08
254	(3, 2)	(1, 8)	(4, 0)	(2, 5)	35.59
338	(3, 3)	(1, 9)	(4, 1)	(2, 6)	39.15

(i.e., $\Delta R = 3.39$ au for Cs). This agrees very well with the results of figure 2(c). Thus, the minima of figures 2(a) and 2(c) are a consequence of the geometry of the system.

Figure 2(b) shows the total energy per atom for the tight-binding model plotted as a function of the size of the cluster. As in figures 2(a) and 2(c) the curve appears to have local minima for regular R-intervals. Here, however, the fact that the size of the cluster cannot be increased continuously but only by complete atomic shells makes the curve of figure 2(b) less smooth than those of figures 2(a) and 2(c). But with some goodwill we may observe local minima for $R = 19.8$, 25.5, 29.7, 34.3, and 37.9 au. The R-spacing for the particularly stable clusters is hence markedly larger than given by equation (7), which points to major differences between the different models. These shall now be explored further.

The similarity of the results of figures 2(a) and 2(c) allows us to focus solely on the spherical-well model when studying the relative stability for larger clusters. Thus, in order to study significantly larger clusters we shall only consider the computationally simpler tight-binding and spherical-well models. In figure 4(a) we show the excess energies for the tight-binding model for clusters with up to 11 017 atoms (including the 161th atomic shell), and in figure 5 the equivalent results for the spherical-well model with up to 31 628 atoms (including 462 electronic (n, l) shells up to $(n, l) = (1, 54)$).

The oscillations in the excess energy in figure 5 are superposed on one with a longer wavelength, so that they almost vanish for $R \simeq 50$ and 85 au. These are the well-known supershells [27, 31], whose occurrence can be explained with the theory of eigenvalue-density oscillations developed by Balian and Bloch [30]. On the other hand, the fact that the curve of figure 5 has a local maximum at around $R \simeq 50$ au and a local minimum at around 150 au is a non-physical consequence of the fitting procedure.

In figure 4 we also show a representation of the spherically symmetric part of the background density of the nuclei and the core electrons. This is obtained by assuming that the density of each nucleus plus the corresponding core can be described by a Gaussian $\left(\alpha/\pi\right)^{3/2} \mathrm{e}^{-\alpha(\vec{r}-\vec{R})^2}$ centred at the site of the nucleus. We use $\alpha = 0.2$ au, corresponding to a full width at half-maximum of 3.72 au.

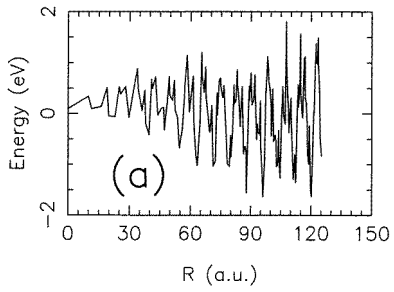

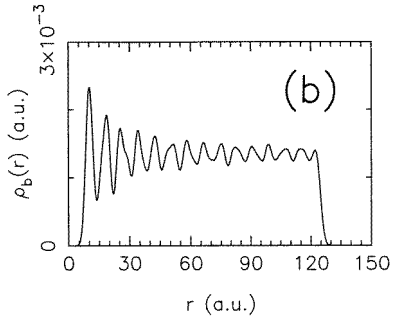

Figure 4. (*a*) The excess energy for the tight-binding model. (*b*) The charge density of the underlying lattice broadened with Gaussians of full width at half-maximum 3.72 au.

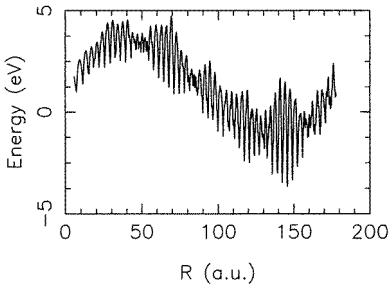

Figure 5. As figure 4(*a*), but for the spherical-well model.

The excess energy of figure 4(*a*) shows well-pronounced minima that are evenly spaced in R consistently with the spacing of figure 2(*b*), i.e., with $\Delta R \simeq 8.06$ au. By comparing with the smeared-out background density of figure 4(*b*) we see that the minima in figure 4(*a*) appear for those values of R for which this background density has local minima. This means that for those clusters where the excess energy is lowest the number of atoms in the vicinity of the surface is low. Thus, the oscillations in figure 4(*a*) are essentially due to surface atoms. Since the number of surface atoms is a property of the crystal structure but independent of the lattice constant, the spacing in ΔR for the local minima of the excess energy will scale with r_s; the present tight-binding model predicts stable clusters for

$$\Delta R \simeq 1.43 r_s. \tag{8}$$

Also for the Hückel and tight-binding models on a truncated fcc crystal, Mansikka-aho *et al* [3] found a strong dependence on surface effects.

In order to be able to study those effects that are not due to the surface we observe that the definition of equation (4) is inappropriate: the number of surface atoms does not simply scale with R^2, as is evident in figure 4(*b*), and it is important to consider the precise number of surface atoms explicitly. We therefore define

$$\tilde{E}_{\rm exc} = E_{\rm tb} - \tilde{a}N - \tilde{b}N_s \tag{9}$$

where N_s is the number of surface atoms. For a given cluster with N_S atomic shells we have let N_s be either the number of atoms of the N_Sth atomic shell or that of the N_Sth and $(N_S - 1)$th atomic shells. Independently of the precise definition used, results such as those of figure 6 are obtained.

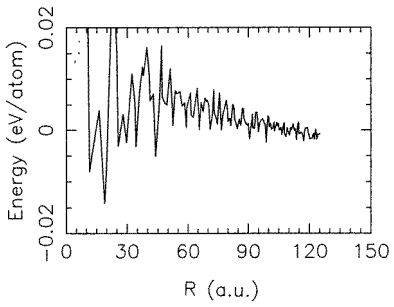

Figure 6. The excess energy of equation (9) for the tight-binding model with the number of surface atoms N_s being the number of atoms in the outermost atomic shell.

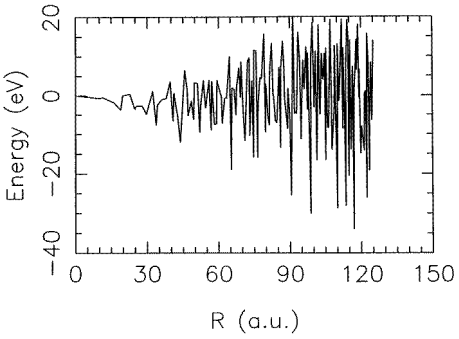

Figure 7. The excess energy of equation (4) for the tight-binding model when including non-zero on-site energies for the surface atoms.

In figure 6 an oscillatory behaviour can be recognized, and on comparing with figure 4(*b*) we see that the R-spacing of the local minima in figure 6 is smaller than that of figure 4(*b*), i.e., about 4 au. Taking all of the approximations into account we find that this agrees reasonably well with the estimate given above (equation (7)) for electronic shells in the spherical well.

A more realistic approach is to treat the surface atoms differently from those of the inner parts of the cluster. Thus, dangling bonds that furthermore might be saturated by surfactants as well as surface reconstructions are likely to cause these orbitals to have different energies from those of the bulk atoms. Accordingly, in the model of section 2.2 the on-site energies t_{ii} for atoms at the surface will be different to those for the others. Ultimately this may remove the surface orbitals from the energy region closest to the Fermi level.

In order to study this proposal we have considered the model of section 2.2 but with t_{ii} arbitrarily set equal to -0.2 eV only for the atoms of the N_Sth atomic shell. Figure 7 shows the results of these calculations. From comparing with figure 4(*b*) it is clear that the excess energy has increased by about one order of magnitude, and one may speculate that the choice above of -0.2 eV is too large. Irrespective of this it is clear that the excess energy of figure 7 has local minima with a periodicity very similar to that observed in figure 6. In total, these results show that the tight-binding model is inappropriate when studying magic numbers, at least when not taking care of the problems related to describing the surface.

3.2. Density of states

In figure 8 we show the DOS for various larger clusters as obtained with the jellium model, and in figure 9 we show that of some larger clusters for the tight-binding model. Finally, figure 10 shows the DOS for the spherical-well model whose general shape is independent of the size of the system. We have therefore not included any Fermi level in figure 10.

The supershells are clearly visible in the results obtained using the spherical-well model (figures 10 and 5), but they only gradually develop for larger clusters within the jellium model. On the other hand, for the largest cluster in figure 8 the energetically lowest supershell gets so smeared out that it hardly is recognizable and the DOS resembles in that energy region mainly that of a free-electron gas, as it should. But also for these largest clusters, the DOS—in particular around the Fermi level—shows large differences compared to that of the crystalline material shown in figure 1.

In contrast to this, the DOS of the tight-binding calculations for N larger than $\sim$2000

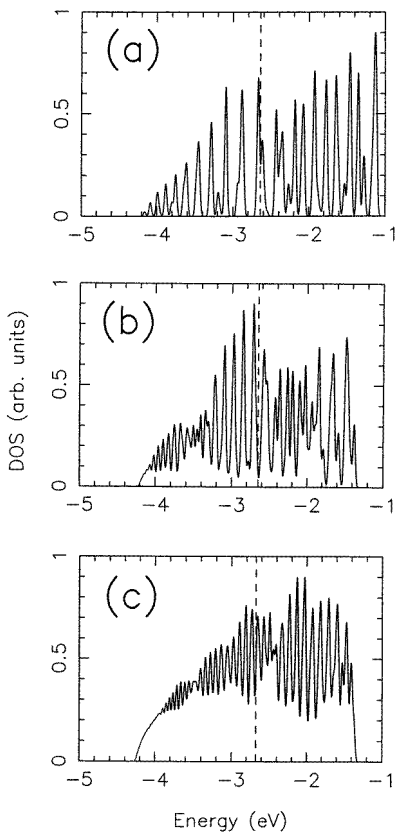

Figure 8. The density of states for clusters with (*a*) $N = 400$, (*b*) $N = 2000$, and (*c*) $N = 9997$ atoms as obtained with the jellium model. The vertical dashed lines mark the Fermi level. All energy levels have been broadened by Gaussians of full width at half-maximum 0.037 eV.

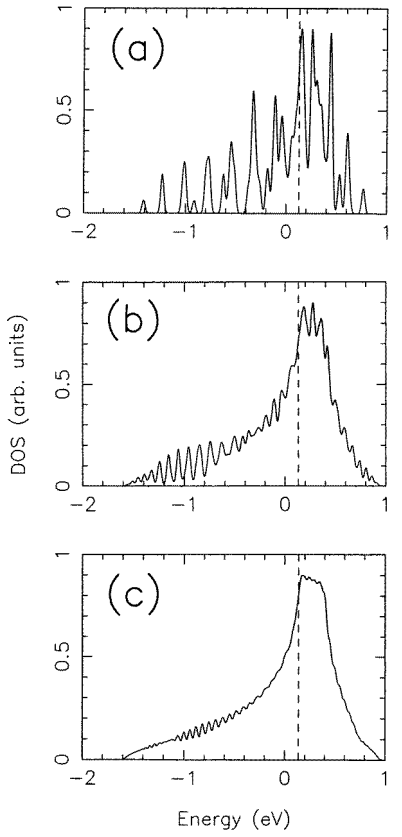

Figure 9. The density of states for clusters with (*a*) $N = 531$, (*b*) $N = 1989$, and (*c*) $N = 11\,017$ atoms as obtained with the tight-binding model. The vertical dashed lines mark the Fermi level. All energy levels have been broadened by Gaussians of full width at half-maximum 0.037 eV.

clearly resembles that of the crystalline material, at least to slightly (∼0.2 eV) above the Fermi level. Thus, both the free-electron-like behaviour at the lowest energies and the local maximum just above the Fermi level are readily recovered for those. This was also found in the simpler Hückel studies for smaller clusters by Lindsay *et al* [5]

For clusters of comparable size the width of the occupied part of the DOS is slightly larger for the tight-binding model than for the jellium model. This may, however, partly be due to the surface states that according to the discussion above appear close to the Fermi level for the tight-binding model and that may occur at slightly higher energies than for the real system.

The results for the jellium model show that for up to about the $\frac{2}{3}N$ lowest levels the results are to a good approximation independent of the cluster size and compare well with those of the spherical-well model. The electrons occupying these levels are accordingly so well localized to the interior of the cluster that they experience a potential that is roughly constant and strongly repulsive on the boundaries.

In contrast to the jellium results, the tight-binding studies give that for a given cluster with N sites only the positions of the local minima in the DOS for up to about $N/2$ electrons can be

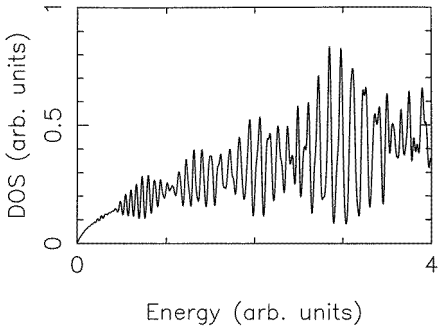

Figure 10. The density of states for the spherical-well model. All energy levels have been broadened by Gaussians of full width at half-maximum 0.037 energy units. Since different clusters only differ by different energy scales, we have not specified the latter; neither have we specified the Fermi level.

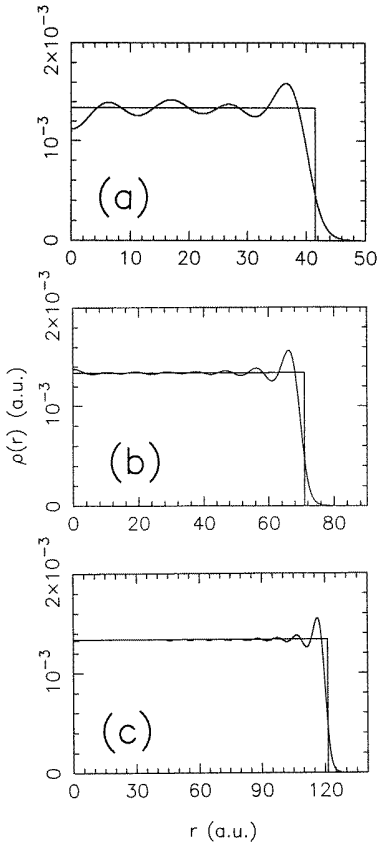

Figure 11. The electron density and background density from the jellium calculations for systems with (*a*) 400, (*b*) 2000, and (*c*) 9997 atoms. The step-like function corresponds to the background density.

considered converged to the values of the jellium and the spherical-well models. This agrees with the Hückel and tight-binding results of Mansikka-aho *et al* [3,4]. They found in addition a relatively strong dependence of the position of the local minima on the truncation (i.e., on the shape of the surface), which once again supports the conclusion that surface effects are important. It turns out that $N/2$ electrons occupy levels up to about 0.5 eV below the Fermi level, which gives an estimate for the energy scale over which surface effects are important.

In the preceding subsection we stressed the importance of the surface atoms and also presented a simple model in which the surface atoms were removed from the vicinity of the Fermi level. Analysing the DOS obtained with this model gives conclusions essentially unchanged from those above.

3.3. Density oscillations

In figure 11 we show some representative examples of the electron density together with the jellium background density from the jellium calculations. The electron density shows a damped

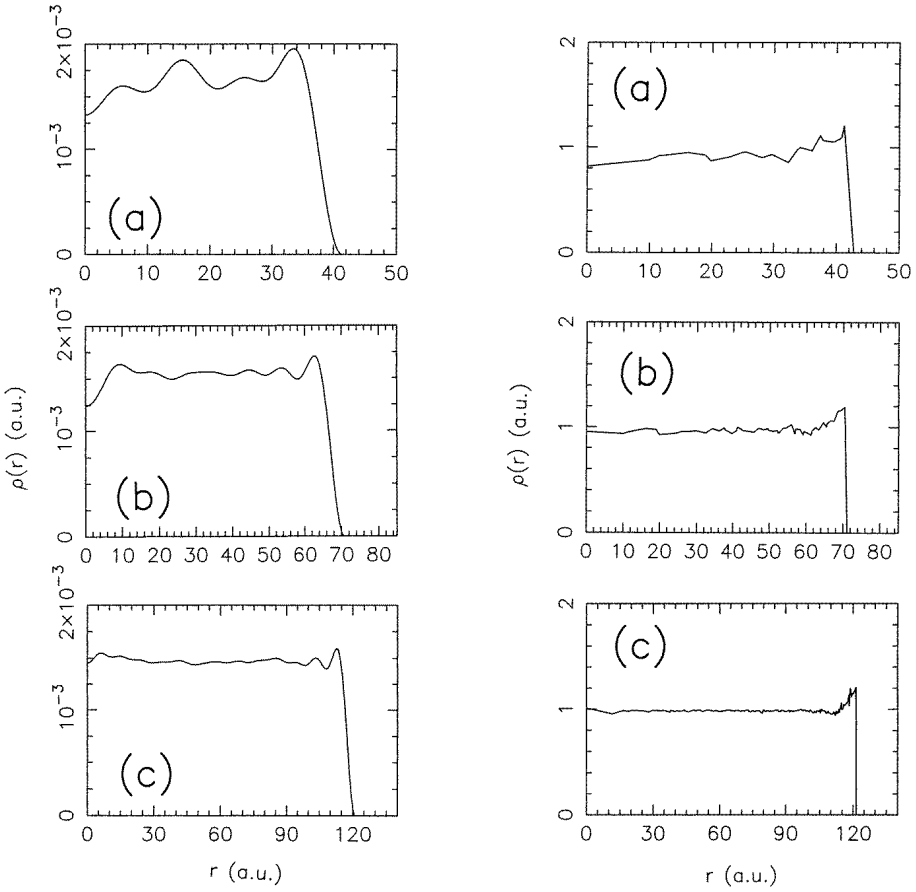

Figure 12. As figure 11, but for the spherical-well model and without the background density. (*c*) corresponds to 10 000 atoms.

Figure 13. Number of electrons per atom as a function of distance from the centre as obtained with the tight-binding model. The panels correspond to clusters with (*a*) 411, (*b*) 1989, and (*c*) 9985 atoms.

oscillatory behaviour with the largest amplitude closest to the surface. For the larger clusters the oscillations are more strongly damped, whereas for the smaller ones (less than $N \sim 1000$ atoms) they prevail throughout the complete system.

In figure 12 we show the same densities as in figure 11 but for the spherical-well model. Also these show an oscillatory behaviour and a convergence towards the constant value for the infinite system, but the oscillations are significant less regular (in particular for the smaller systems), and the maximum does not always occur close to the surface. The main difference between the two models is the electron–electron interactions that are present in the jellium model but absent in the spherical-well model.

Within the jellium model we have assumed that the electrons move in the field of a homogeneous background density and that they are essentially confined to a spherical part of space. Another way of confining the electrons is to introduce a repulsive spherical potential shell in an infinite, homogeneous jellium. It is well known (see, e.g., reference [32]) that a potential of the form $V_0\delta(\vec{r})$ placed in an otherwise infinite, homogeneous jellium produces an oscillatory electron density superposed on the otherwise constant density. The spherical

potential shell can be interpreted as a superposition of point potentials, resulting in the following oscillatory part of the density [33]:

$$\delta\rho(\vec{r}) = -2V_0k_F^2\frac{m}{h^2}\frac{R_0}{r}\left\{f[2k_F(R_0-r)] - f[2k_F(R_0+r)]\right\}. \tag{10}$$

Here,

$$k_F = \left(\frac{9\pi}{4}\right)^{1/3}\frac{1}{r_s} \simeq \frac{1.92}{r_s} \tag{11}$$

is the Fermi momentum and R_0 is the radius of the potential sphere. R_0 is supposed to be larger than R since the electron density of the jellium model for the clusters has a tail sticking out of the jellium. The function $f(x)$ is given by

$$f(x) = \frac{\sin x}{x^2} - \frac{\cos x}{x} + \frac{\pi}{2} - \mathrm{Si}(x) \tag{12}$$

with Si being the sine integral. f is an oscillating and decaying function. Thus, the electron density oscillates with a wavelength of

$$\lambda_F = \frac{\pi}{k_F} \simeq 1.636r_s. \tag{13}$$

For Cs, $\lambda_F = 9.19$ au.

One may speculate on whether the density oscillations have any influence on the stability of the clusters. The two f-functions in equation (12) interfere constructively whenever R is increased by $\lambda_F/2$, i.e. by

$$\Delta R \simeq 0.818r_s \tag{14}$$

which equals 4.60 au for the Cs clusters. This ΔR spacing, however, does not coincide with those observed in jellium studies of the stability of clusters and we therefore conclude that these density oscillations are only at most of secondary importance for the stability of the clusters.

For the tight-binding model each orbital is a linear combination of all atomic basis functions,

$$\psi_i = \sum_{\vec{R}} c_{i,\vec{R}}\phi_{\vec{R}}. \tag{15}$$

Subsequently, we define

$$\rho(R) = \frac{1}{N(R)}\sum_i\sum_{\vec{R}'}\delta_{R,R'}|c_{i,\vec{R}'}|^2 \tag{16}$$

where the $\vec{R}'$-summation is only over those sites that are at exactly the distance R from the centre, and $N(R)$ is their number.

This density is shown in figure 13 for approximately the same cluster sizes as those of figure 11 for the jellium model and of figure 12 for the spherical-well model. The results show that the density has a local maximum close to the surface independently of the size of the system and which resembles what was found in figures 11 and 12 for the other two models. On the other hand, Friedel oscillations such as those of figure 11 are only marginally resolved, so the true electron density will be dominated by the underlying lattice structure (since $\rho(R)$ of equation (16) will be modulated by the background density of figure 4(*b*)). At this point it should be added that originally the Friedel oscillations were found when considering the response of an infinite, homogeneous electron gas to a point perturbation. Therefore, when using the infinite system as a starting point, it is important that the model includes a

proper description of screening which for the present models is only the case for the jellium model. However, when including the perturbation (either the point potential or the spherical confinement) right from the start, all models should, in the ideal case, give the same results.

The differences between figures 11, 12, and 13 show that without support from other sources (experiment or more exact theoretical studies) none of the methods can be considered reliable in describing this property. It should be stressed here that the spherical-well model is clearly a simplified model compared with the other two, but as regards the other two there is no reason to consider one superior to the other. That these two predict different behaviours must therefore be considered disturbing.

In each of the figures 11, 12, and 13 it is seen that the electron density at the centre of the cluster oscillates with cluster size. However, the oscillations of the three models do not follow the same pattern.

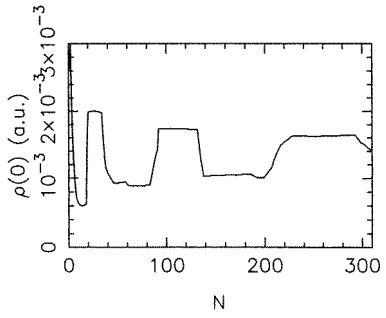

Figure 14. The electron density at the centre of the cluster as a function of the number of atoms N in the cluster as calculated with the jellium model.

For the large jellium systems we may use equations (10) and (12) to calculate the density at the centre [33]:

$$\delta\rho(0) = -2V_0k_F\frac{m}{h^2}\frac{1}{R_0}\left[\frac{\sin(2k_FR_0)}{2k_FR_0} - \cos(2k_FR_0)\right] \sim j_1(2k_FR_0). \qquad (17)$$

As a function of cluster size, this density shows oscillations with local maxima separated by the wavelength of equation (13). The jellium calculations for the smaller clusters (up to 310 atoms) predict, however, a somewhat different behaviour (figure 14). Thus, the density at the centre is, according to these, roughly piecewise constant. It increases whenever an s level is being filled in agreement with the results of the spherical-well model, but when the cluster is subsequently enlarged without new s levels being filled, the density does not decrease until a certain size is reached when a new s level gets filled. This means that the reduction in this density that should accompany the increased size is compensated by other effects. It is moreover remarkable that those cluster sizes for which the density at the centre drops are those for which p levels are being filled; cf. table 1. (Note that in table 1 more shells are filled roughly simultaneously for the larger systems. However, they are filled in the order given in the table, so, e.g., for the systems with N between 186 and 254 the $l = 0$ shell is filled for N roughly between 230 and 232). The reason for the reduction in the density at the centre when a p shell is being filled may be the following. After the s orbitals, the p orbitals are those with the largest density closest to the centre. Therefore, when the p shells are being filled, the s electrons are being expelled from the central region, giving a reduction in the electron density at the centre.

4. The clusters with a void

Recently, it has been shown experimentally [33, 34] that it is possible to deposit layers of metal atoms on the exterior of a C_{60} molecule. Although there will be chemical interactions between the buckyball and the metal atoms one may to a first approximation assume that the resulting system can be considered a metal cluster with a void at the centre. Thus, for those metals for which the magic numbers of the pure clusters (i.e., without a void) are determined by the closing of electronic shells one may suggest that the same is the case for the clusters with a void. Cs belongs to this group. For Cs one further aspect is important: the electronic hopping integrals (cf. section 2.2) are more than one order of magnitude smaller than those for the frontier orbitals of the C_{60} molecule. And since the C_{60} molecule has a gap around the Fermi level, the frontier orbitals of the Cs-covered buckyball are largely localized to the Cs atoms, so the closing of electronic shells is mainly dictated by properties of the metal.

A further argument for considering this simple model comes from an earlier study [33] where it was shown that the magic numbers of the Cs-covered C_{60} could be reasonably well described by using a jellium model with a void at the centre. In that study it was important to take into account that six electrons were transferred from the metal to the C_{60} molecule.

In the present study we shall focus on the changes in the electronic and stability properties of the Cs clusters when they have a void at the centre. As a possible realization of these systems we shall have metal-covered C_{60} in mind, but we shall not attempt here to make any further comparison with the experimental results. We shall therefore not study the effects of removing a number of electrons from the metal but assume that the cluster with the void has as many electrons as atoms.

Table 2. As table 1, but for the jellium with a void at the centre. R is the outer radius of the jellium calculated from equation (18).

N	(n, l)				R (au)
2	(1, 0)				9.90
8	(1, 1)				12.67
18	(1, 2)				15.62
32	(1, 3)				18.46
52	(1, 4)	(2, 0)			21.43
58	(2, 1)				22.18
90	(1, 5)	(2, 2)			25.50
130	(1, 6)	(2, 3)			28.72
186	(3, 0)	(1, 7)	(2, 4)	(3, 1)	32.28
252	(3, 2)	(1, 8)	(2, 5)		35.66
332	(3, 3)	(1, 9)	(2, 6)	(4, 0)	39.05
428	(1, 10)	(3, 4)	(2, 7)	(4, 1)	42.47

Within the jellium model the void is assumed to have a radius of $R_C = 8.50$ au, so the outer radius of the jellium becomes

$$R = \left(Nr_s^3 + R_C^3\right)^{1/3}. \tag{18}$$

In table 2 we show the properties of the magic clusters of this model, analogously to table 1 for the jellium without a void. From comparing with table 1 it is obvious that the two systems show only small differences and these are largest for the smallest clusters, which should not surprise. For the larger clusters, the magic numbers seem to be slightly smaller for the cluster with a void than for that without. It is interesting to notice that thereby the R-values of the closed-shell clusters of the two systems become more similar, which is only possible by having

a slightly different ordering of the (n, l) shells. But the similarity of the two systems shows also that the (spherical) symmetry is the overall driving factor dictating the magic numbers.

The presence of the void means that it becomes energetically unfavourable for the electrons to be in that region. Within the tight-binding model we may accordingly use two different approaches in modelling the presence of the void: either simply removing the central atoms or giving these on-site energies well above those of the other atoms. In the latter case one should also reduce the total number of electrons. Here, we have chosen to use the second approach, but on choosing the values of these on-site energies equal to 10 eV the two approaches become essentially identical. Furthermore, from our results of section 3.1 we learned that surface effects may obscure our results, so therefore we included extra on-site energies for the surface atoms (equal to -0.2 eV as in figure 7). The void was supposed to occupy the region of the central atom and the first atomic shell (in total nine atoms).

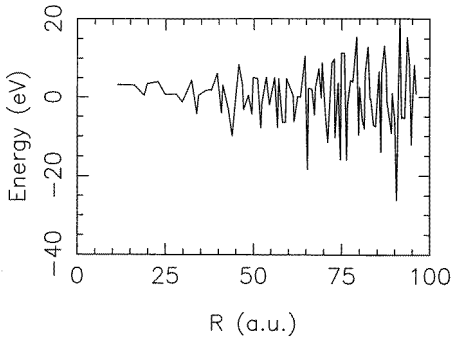

Figure 15. As figure 7, but for the system with a void.

In figure 15 we show the results for clusters of up to about 5000 atoms equivalent to those of figure 7 for the pure system without a void. Comparing the two systems we observe only very small differences. This result is less trivial than it at a first sight may appear, since for a given R the number of electrons is different (by 9), whereas the number of atoms is unchanged. The largest differences are found for the systems with R up to about 25 au, in agreement with the findings for the jellium model.

We shall use the spherical-well model in analysing these systems. The single-particle energies are here obtained by replacing equation (6) by the two equations

$$\begin{aligned} c^j_{nl} j_l\left(\sqrt{\frac{2m}{\hbar^2}\epsilon_{nl}}R_C\right) + c^y_{nl} y_l\left(\sqrt{\frac{2m}{\hbar^2}\epsilon_{nl}}R_C\right) &= 0 \\ c^j_{nl} j_l\left(\sqrt{\frac{2m}{\hbar^2}\epsilon_{nl}}R\right) + c^y_{nl} y_l\left(\sqrt{\frac{2m}{\hbar^2}\epsilon_{nl}}R\right) &= 0 \end{aligned} \tag{19}$$

where y_l is the lth spherical Bessel function of the second kind, and where R is obtained from equation (18).

For $l = 0$ equation (19) reduces to

$$\epsilon_{n0} = \frac{n^2\hbar^2\pi^2}{2m(R - R_C)^2} \tag{20}$$

which is the same expression as that for the spherical well without the void at the centre, except that for the latter R_C has to be replaced by 0. This explains why the energy spacing between the orbitals with $l = 0$ is much larger for the system of this section than for that without the void at the centre. Therefore, with the void some of the (n, l) shells with $n = 1$ but higher l become filled before the $(2, 0)$ shell unlike in the model without the void. This confinement

effect explains the main differences between the results for the system with the void and those for the system without the void.

The present spherical-well model possesses one further difference from that of the previous section. In the latter case the (n, l) shells were ordered in a universal order independent of N, and the only N-dependence was through a rescaling of the energies. But with the void the (n, l) shells change their relative order as a function of N.

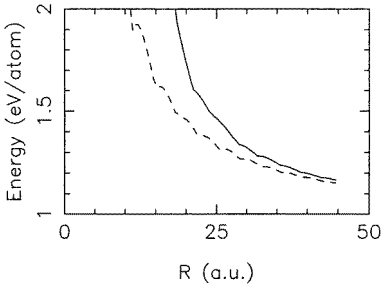

Figure 16. The energy per atom for the spherical-well model as a function of the radius of the system. The full curve corresponds to the system with a void at the centre and the dashed one to that without a void. Systems with up to 500 atoms are included.

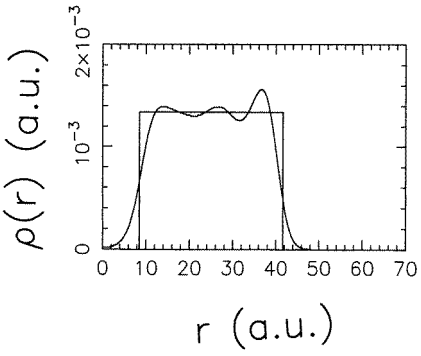

Figure 17. As figure 11(a), but for a system with a void at the centre.

In figure 16 we show the energy per electron for the present spherical-well model as a function of the radius R of equation (18) for $R_C = 8.5$ au for up to $N = 500$ atoms. For the sake of comparison we also show the similar results for the system without the void. We see first of all that the radial confinement for the system with the void leads to a higher energy than that for the system without the void (cf., the discussion above), but also that for the larger systems the two energies approach each other, as expected. The results obtained using the spherical-well model of figure 16 differ only slightly from those of the jellium calculations (table 2).

We may for the system with a void, equivalently to section 3.3, model the confinement of the electrons as being due to two concentric spherical repulsive potential shells, of which one is equivalent to the one of section 3.3 and the other keeps the electrons outside the region of the void. However, just as for the former model we will allow the electrons to have a tail sticking out of the cluster jellium region, so the radius of the inner sphere is supposed to be $R_c < R_C$ just as $R_0 > R$. This leads to an oscillating part of the electron density equal to [33]

$$\delta\rho(\vec{r}) = -2V_0k_F^2\frac{m}{h^2}\frac{R_c}{r}\left\{f[2k_F(r-R_c)] - f[2k_F(r+R_c)]\right\} \\ -2V_0k_F^2\frac{m}{h^2}\frac{R_0}{r}\left\{f[2k_F(R_0-r)] - f[2k_F(R_0+r)]\right\} \qquad (21)$$

with $f(x)$ given by equation (12). The second term is the same as in equation (10) and is due to the outer confining potential, whereas the first term is due to the inner confining potential.

In figure 17 we show one example of the electron density from the jellium calculations for a system with $N = 400$ atoms. Comparing figures 11(a) and 17 we see that the two outermost maxima in $\rho(r)$ in figure 17 are as those in figure 11(a) although slightly displaced, whereas the third maximum does not have a counterpart in figure 11(a) at that position. This last one is

obviously caused by the inner potential shell and at that position the first term in equation (21) dominates strongly over the second one.

5. Conclusions

In the present work we have applied three different models for studying the ground-state properties of Cs_N clusters. We have in particular focused on similarities of and differences between the predictions of the three models and thereby identified properties that are model dependent and where experimental studies can be useful in evaluating the quality of the different models or, alternatively, where the models can be applied only with caution in explaining the experimental results. We have also been able to identify different length scales that are relevant for the magic numbers, surface effects, and Friedel oscillations.

We found that the spherical symmetry was the overall driving factor producing the closed shells. Thus, the magic numbers as defined through equation (7) are found for all three models. When introducing a void at the centre, equation (7) remained valid, which could only be achieved by slightly rearranging the order in which the (n, l) shells were filled. However, for the tight-binding model we found that surface effects could obscure the results. These led to possible extra features as given by equation (8). But it is not unlikely that the surface atoms have to be treated differently from the other atoms, and by assuming this to be the case we could recover the stability oscillations as given by equation (7).

The densities of states for the lowest parts of the occupied orbitals were very similar for all three models and resembled that of a free-electron gas for not too small systems. However, the densities of states around the Fermi level showed differences, where only the tight-binding model could be made to converge (as a function of $N \to \infty$) to that of the infinite crystal. Therefore, neither the spherical-well model nor the jellium model appears to be appropriate when studying low-energy single-particle excitations.

All three models showed clear indications of the occurrence of supershells. The models differed, however, in the predictions of where the nodes of these should occur. This is understandable if one notices that these are very sensitive to surface effects that are clearly described differently in the three models.

The fact that the electrons feel each other's presence could hardly be noticed in the relative stability of the clusters. It could, however, be seen in the electron density of the individual clusters. Here, the electron density of the jellium model showed a much more regular behaviour with well-developed Friedel oscillations than was the case for the other models. Furthermore, for the pure clusters without a void the densities and potentials at the centre were particularly simple to calculate, and they were markedly different for the jellium model than what would be obtained with the spherical-well model. In particular we mention the surprising finding from the jellium model that the electron density at the centre is roughly piecewise constant as a function of N and only goes up when s shells are being filled or down when p shells are being filled. We argued that the behaviour of the s and p orbitals closest to the centre could explain these findings at least partly.

In total our study has shown that the sizes of the particularly stable clusters are described equivalently by all three models, as long as care is taken in the treatment of surface atoms within the tight-binding model. Therefore, studies of the magic numbers cannot be used in discriminating between the different models. Moreover, for the densities of states of the occupied orbitals of the Cs_N clusters the three models also yield similar results. However, when looking at the finer details of these, in particular around the Fermi level, differences are found. Therefore, one has to be well aware of the limitations and possibilities of the three models when applying them for interpreting low-energy excitations or optical properties.

Furthermore, the electron densities of equivalent clusters were markedly differently described by the three models. Therefore, more detailed experimental studies on size-selected clusters would be very useful in estimating the quality of the different models.

Finally, surprisingly similar results were obtained independently of whether or not the systems contained a void at the centre. In particular, the magic numbers and the electron densities were described by the same length scales for the two types of system.

Acknowledgments

The author acknowledges very useful discussions with Erich Koch, Sashi Satpathy, and Karla Schmidt, and is grateful to an anonymous referee for some very useful comments. Generous financial support from Fonds der Chemischen Industrie is gratefully acknowledged.

References

[1] de Heer W A 1993 *Rev. Mod. Phys.* **65** 611
[2] Brack M 1993 *Rev. Mod. Phys.* **65** 677
[3] Mansikka-aho J, Manninen M and Hammarén E 1991 *Z. Phys.* D **21** 271
[4] Mansikka-aho J, Manninen M and Hammarén E 1994 *Z. Phys.* D **31** 253
[5] Lindsay D M, Wang Y and George T F 1990 *J. Cluster Sci.* **1** 107
[6] Cini M 1975 *J. Catal.* **37** 187
[7] Martins J L, Car R and Buttet J 1981 *Surf. Sci.* **106** 265
[8] Beck D E 1984 *Solid State Commun.* **49** 381
[9] Beck D E 1984 *Phys. Rev.* B **30** 6935
[10] Ekardt W 1984 *Phys. Rev. Lett.* **52** 1925
[11] Ekardt W 1984 *Phys. Rev.* B **29** 1558
[12] Puska M J, Nieminen R M and Manninen M 1985 *Phys. Rev.* B **31** 3486
[13] Koch E 1996 *Phys. Rev. Lett.* **76** 2678
[14] Koch E and Gunnarsson O 1996 *Phys. Rev.* B **54** 5168
[15] Genzken O, Brack M, Chabanat E and Meyer J 1992 *Ber. Bunsenges. Phys. Chem.* **96** 1217
[16] Genzken O and Brack M 1991 *Phys. Rev. Lett.* **67** 3286
[17] Brack M, Genzken O and Hansen K 1991 *Z. Phys.* D **21** 65
[18] Chou M Y, Cleland A and Cohen M L 1984 *Solid State Commun.* **52** 645
[19] Hohenberg P and Kohn W 1964 *Phys. Rev.* **136** B864
[20] Kohn W and Sham L J 1965 *Phys. Rev.* **140** A1133
[21] Lermé J, Pellarin M, Baguenard B, Bordas C, Vialle J L and Broyer M 1994 *Phys. Rev.* B **50** 5558
[22] Ekardt W, Tran Thoai D B, Frank F and Schulze W 1983 *Solid State Commun.* **46** 571
[23] Knight W D, Clemenger K, de Heer W A, Saunders W A, Chou M Y and Cohen M L 1984 *Phys. Rev. Lett.* **52** 2141
[24] Clemenger K 1991 *Phys. Rev.* B **44** 12 991
[25] Lermé J, Bordas Ch, Pellarin M, Baguenard B, Vialle J L and Broyer M 1993 *Phys. Rev.* B **48** 9028
[26] Catara F, Chomaz Ph and Van Giai N 1995 *Z. Phys.* D **33** 219
[27] Nishioka H, Hansen K and Mottelson B R 1990 *Phys. Rev.* B **42** 9377
[28] von Barth U and Hedin L 1972 *J. Phys. C: Solid State Phys.* **5** 1629
[29] Andersen O K 1975 *Phys. Rev.* B **12** 3060
[30] Balian R and Bloch C 1972 *Ann. Phys., NY* **69** 76
[31] Pedersen J, Bjørnholm S, Borggren J, Hansen K, Martin T P and Rasmussen H D 1991 *Nature* **353** 733
[32] Ashcroft N W and Mermin N D 1976 *Solid State Physics* (Philadelphia, PA: Saunders College)
[33] Springborg M, Satpathy S, Malinowski N, Zimmermann U and Martin T P 1996 *Phys. Rev. Lett.* **77** 1127
[34] Martin T P, Malinowski N, Zimmermann U, Näher U and Schaber H 1993 *J. Chem. Phys.* **99** 4210